

FIG. 3 Expression of midbrain-hindbrain markers in 10.5 d.p.c. embryos. *Pax-5* (a–c), *Wnt-1* (d–f) and *Fgf-8* (g–i) expression was visualized by whole-mount *in situ* hybridization and both *En-1* and *En-2* expression (j–l) by antibody staining. Representative examples of wild-type (a, d, g, j; +/+; non-Tg) and *Wnt-1* mutants (b, e, h, k; –/–; non-Tg) which do not carry the transgene and *Wnt-1* mutants carrying the transgene (c, f, i, l; –/–; Tg) are shown. No alteration in the normal expression pattern of any of the markers was observed in wild-type embryos expressing the transgene.

ref. 1) pups were genotyped at 10 days post partum ( $n = 68$ ), but no live *Wnt-1*<sup>–/–</sup>; *WEXPZ-En-1*<sup>+</sup> mice were obtained, so *En-1* was insufficient to rescue the *Wnt-1*-null phenotype completely. Further analysis indicated that between 14.5 and 18.5 d.p.c., brains of *Wnt-1*<sup>–/–</sup>; *WEXPZ-En-1*<sup>+</sup> embryos deteriorate (data not shown). Thus there may be additional functions of *Wnt-1* signalling that cannot be replaced by *En-1*. This conclusion is supported by analysis of two cranial motor nerves, III (oculomotor) and IV (trochlear), which normally develop adjacent to *Wnt-1*-expressing cells in the ventral midbrain. Each of these fail to develop in *Wnt-1*<sup>–/–</sup> embryos<sup>21</sup>. Similarly, neither nerve forms in *Wnt-1*<sup>–/–</sup>; *WEXPZ-En-1*<sup>+</sup> embryos which have global restoration of midbrain development (data not shown). In contrast, we have found that a second ventral population, tyrosine-hydroxylase-expressing neurons (catecholaminergic neurons) of the substantia nigra are rescued in *Wnt-1*<sup>–/–</sup>; *WEXPZ-En-1*<sup>+</sup> embryos (data not shown).

In summary, in the absence of a *Wnt-1* signal, expression of *En-1* from the *Wnt-1* enhancer is sufficient to substantially rescue early midbrain and anterior hindbrain development. These results suggest that a major role of *Wnt-1* signalling in the mammalian brain is to maintain *En* expression. This is identical to a role proposed for *Wingless* signalling in the *Drosophila* epidermis, demonstrating that this aspect of the regulatory pathway has been conserved from flies to mice. □

## Methods

**Transgenic mice.** The expression vector pWEXPZ-*En-1* contains the *En-1* cDNA and an 825-base-pair piece of *E. coli lacZ* as an mRNA tag (hatched box in Fig. 1f) inserted at the *EcoRV* site of pWEXP2 (ref. 14). Filled and shaded boxes in Fig. 1f represent translated and untranslated parts of *Wnt-1* exons,

respectively. Transgenic lines were generated essentially as described<sup>14</sup>. Nine transmitting founder lines were generated, three of which expressed the transgene appropriately in embryos. These were crossed with *Wnt-1*<sup>+/-</sup> mice<sup>1</sup> to generate *Wnt-1*<sup>+/-</sup>; *WEXPZ-En-1*<sup>+</sup> males. Expression of *En-1* from the transgene resulted in severe hydrocephalus and lethality in three founder mice and in transgenic offspring of two expressing founders (data not shown) but one line was stably maintained on the *Wnt-1*<sup>+/-</sup> background. Southern blotting of yolk-sac DNA was done described<sup>22</sup> using the probe described<sup>4</sup>.

**Whole-mount *in situ* hybridization.** This was done with digoxigenin-labelled probes as described<sup>15</sup> and modified according to ref. 23. *Pax-5*<sup>16</sup>, *Wnt-1*<sup>15</sup> and *Fgf-8*<sup>18</sup> probes have been described. The probe used to detect *Wnt-1* mRNA also detects transgene mRNA. The transgene-specific probe was generated from the *lacZ* tag in pWEXPZ-*En-1*.

**Whole-mount antibody staining.** Expression of *En-1* and *En-2* proteins was detected by whole-mount antibody staining using the polyclonal antiserum  $\alpha$ Enhb-1, which recognizes both proteins<sup>20</sup>.

**Histological analysis.** Embryos were collected in PBS, fixed in Bouin's fixative, dehydrated, embedded in wax and sectioned at 6  $\mu$ m. Sections were dewaxed, rehydrated and stained with haematoxylin and eosin.

Received 3 June; accepted 29 July 1996.

- McMahon, A. P. & Bradley, A. *Cell* **62**, 1073–1085 (1990).
- Thomas, K. R. & Capecchi, M. R. *Nature* **346**, 847–850 (1990).
- Davis, C. A. & Joyner, A. L. *Genes Dev.* **2**, 1736–1744 (1988).
- McMahon, A. P., Joyner, A. L., Bradley, A. & McMahon, J. A. *Cell* **69**, 581–595 (1992).
- DiNardo, S., Sher, E., Heemskerk-Jongens, J., Kassis, J. & O'Farrell, P. *Nature* **332**, 604–609 (1988).
- Martinez-Arias, A., Baker, N. E. & Ingham, P. W. *Development* **103**, 157–170 (1988).
- Heemskerk, J., DiNardo, S. & Kostriken, R. *Nature* **352**, 404–410 (1991).
- Ingham, P. W. & Martinez Areas, A. *Cell* **68**, 221–235 (1992).
- Klingensmith, J. & Nusse, R. *Dev. Biol.* **170**, 636–650 (1995).
- Rowitz, D. H. & McMahon, A. P. *Mech. Dev.* **52**, 3–8 (1995).
- Mastick, G. S. et al. *J. Comp. Neurol.* (in the press).
- Wurst, W., Auerbach, A. B. & Joyner, A. L. *Development* **120**, 2065–2075 (1994).
- Joyner, A. L. et al. *Science* **251**, 1239–1243 (1991).
- Echelard, Y. et al. *Cell* **75**, 1417–1430 (1993).
- Parr, B., Shea, M., Vassileva, G. & McMahon, A. P. *Development* **119**, 247–261 (1993).
- Asano, M. & Gruss, P. *Mech. Dev.* **39**, 29–39 (1992).
- Crossley, P. H. & Martin, G. R. *Development* **121**, 439–451 (1995).
- Mahmood, R. et al. *Curr. Biol.* **5**, 797–806 (1995).
- Crossley, P. H., Martinez, S. & Martin, G. R. *Nature* **380**, 66–68 (1996).
- Davis, C. A., Holmyard, D. P., Millen, K. J. & Joyner, A. L. *Development* **111**, 287–298 (1991).
- Fritzsche, B., Nichols, D. H., Echelard, Y. & McMahon, A. P. *J. Neurobiol.* **27**, 457–469 (1995).
- Takada, S. et al. *Genes Dev.* **8**, 174–189 (1994).
- Knecht, A. K., Good, P. J., Dawid, I. B. & Harland, R. M. *Development* **121**, 1927–1936 (1995).

ACKNOWLEDGEMENTS. We thank B. Klumppar for sectioning, A. Joyner for *En-1* cDNA and  $\alpha$ Enhb-1 antiserum, M. Busslinger for *Pax-5* cDNA, C. Dickson for *Fgf-8* cDNA, our colleagues for their comments on the manuscript, and W. Wurst and A. Joyner for sharing unpublished results. This work was supported by grants from the NIH to A.P.M. and by a postdoctoral fellowship from the Human Frontiers Science Program to P.S.D.

CORRESPONDENCE and requests for materials should be addressed to A.P.M. (e-mail: amcmahon@hubio2.harvard.edu).

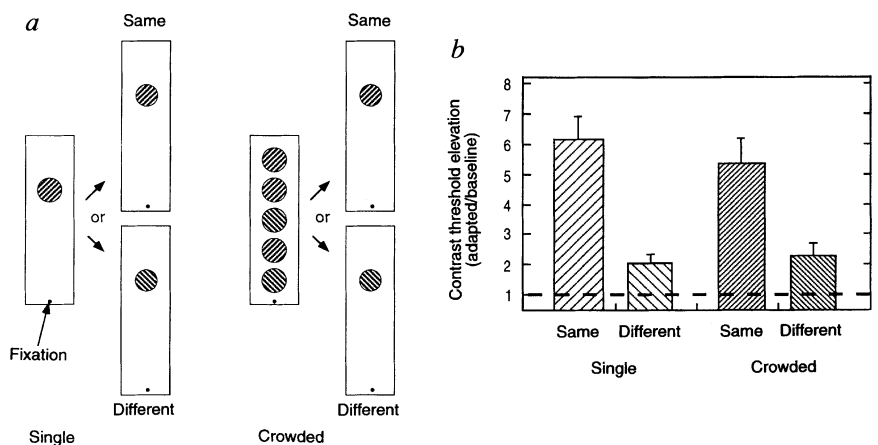
## Attentional resolution and the locus of visual awareness

Sheng He, Patrick Cavanagh & James Intriligator

Department of Psychology, Harvard University, Cambridge, Massachusetts 02138, USA

**VISUAL spatial resolution is limited by factors ranging from optics to neuronal filters in the visual cortex<sup>1,2</sup>, but it is not known to what extent it is also limited by the resolving power of attention. To investigate this, we studied adaptation to lines of specific orientation, a process that occurs in primary visual cortex<sup>3</sup>. When a single grating is presented in the periphery of the visual field, human observers are aware of its orientation, but when it is flanked by other similar gratings ('crowding'), its orientation becomes impossible to discern<sup>4,5</sup>. Nevertheless, we show that orientation-specific adaptation is not affected by crowding, implying that spatial resolution is limited by an attentional filter acting beyond the primary visual cortex. Consistent with this, we find that attentional resolution is greater in the lower**

FIG. 1 Orientation-selective adaptation when subjects could and could not perceive the orientation of the adapting grating (fourth grating from the fixation point). In all experiments, stimuli were circular patches of sinusoidal gratings. *a*, Contrast thresholds were measured for three conditions: adapted to a single grating; adapted to the fourth stimulus in a linear array of five; no adaptation (baseline). The adapting grating and test grating were centred  $25^\circ$  above the point of visual fixation. The radius for each grating was  $2.67^\circ$ , and the centre-to-centre distance between neighbouring gratings was  $6.67^\circ$ . Except in the baseline condition, subjects were exposed to a continuous 5-s adaptation, 300-ms interstimulus interval, 180-ms test cycle, during which threshold contrast for the test grating was set by the subjects. Settings were not recorded during the first 10 cycles to ensure that subjects could achieve a stable adapted state. For each adapting–testing cycle, the orientation of the first grating was randomly chosen to be either  $45^\circ$  or  $135^\circ$ , and the orientation of the other distractors were successively rotated by  $90^\circ$ . Orientation of the fourth target grating was predetermined and remained the same for each session. *b*, Threshold contrast elevation after adaptation, compared with baseline contrast threshold before adaptation. Mean of four subjects; error bars show s.e.m. The difference between



same adapt–test orientation and different adapt–test orientation represents the strength of orientation selective adaptation. The data show that a flanked grating (orientation not perceivable) and a single grating (orientation readily perceivable) were almost equally effective in orientation-specific adaptation.

than in the upper visual field, whereas there is no corresponding asymmetry in the primary visual cortex. We suggest that the attentional filter acts in one or more higher visual cortical areas to restrict the availability of visual information to conscious awareness<sup>6</sup>.

A high-contrast adapting grating patch of one cycle per degree was presented  $25^\circ$  above the point of visual fixation. When presented alone, the orientation of the grating was clearly visible even at contrasts of less than 10%. When the same adapting grating was presented fourth in a linear array of five similar grating patches (maximizing the crowding effect<sup>5,7</sup>), subjects identified the orientation at chance levels, even with unlimited viewing time at full contrast (Fig. 1*a*). We tested whether there was any orientation-specific analysis of the grating when the subjects were unaware of the orientation. Observers were adapted to a target grating presented alone or with flanking gratings (one above and three below the target), and then were tested on their ability to identify the orientation of a grating either at the same or orthogonal orientation presented at the target position (Fig. 1*a*). When observers were adapted to a crowded grating (and were unaware of its orientation), the contrast thresholds in tests in which the grating was of the same orientation as the adapting grating were roughly 2 to 3 times higher than for tests using the orthogonal orientation (see Fig. 1*b*). We found this same orientation-specific threshold elevation when observers were adapted to

a single grating, and were aware of its orientation. There is a clear dissociation between perceptual awareness of orientation and orientation-specific adaptation (located at or beyond the primary visual cortex (area V1), the first site of orientation processing). The results indicate that visual awareness, and the 'crowding' that blocks it, occur after orientation analysis in the visual information processing stream. Others have reported that unresolvable high-frequency gratings can produce orientation-specific adaptation<sup>2</sup>, and orientation information can be used for segmentation without the explicit knowledge of the subject<sup>8</sup>. Our results indicate further that activation of neurons in V1 is insufficient for conscious perception<sup>6</sup>.

Conventionally, the reduced sensitivity to targets embedded in a field of similar items is termed 'lateral masking' and is often attributed to lateral inhibition between neighbouring neurons at early stages of processing<sup>9</sup>. We show that the information that is inaccessible to perceptual awareness because of crowding, is in fact processed by the primary visual cortex without disruption, ruling out the simplest sensory lateral masking explanation. We believe that this crowding effect reflects the limited resolution of the spatial attention mechanism.

The crowding effect seemed stronger in the upper visual field than in the lower field. Lesion<sup>10</sup> and functional magnetic resonance imaging (fMRI)<sup>11,12</sup> studies show that human primary visual cortex devotes roughly the same area to the representations of the

FIG. 2 Discrimination of grating orientation. *a*, Examples of four stimulus conditions. All gratings were 1 cycle per degree. Grating patches had a  $2^\circ$  radius, and the centre of the target grating was  $20^\circ$  from the point of fixation. In the crowding condition, the centre-to-centre distance between neighbouring gratings was  $5^\circ$ . Stimuli were presented for 180 ms. Subjects were instructed to always report (and hence attend to) only the orientation of the grating patch in the middle, ignoring the flanking gratings when they appeared. Visual field positions were fixed during each session, and varied between sessions. Stimuli were presented at 4 different contrast levels (target and flanking stimuli always had the same contrast). *b*, Mean  $\pm$  s.e.m. accuracy from three subjects. Symbols correspond to the conditions depicted in *a*. Whereas subjects could see the grating orientation almost equally well in both the upper and lower visual field (open symbols), their ability to identify the orientation of the target grating was much more affected by flanking stimuli when presented in the upper visual field (filled triangles) than in the lower visual field (filled circles).

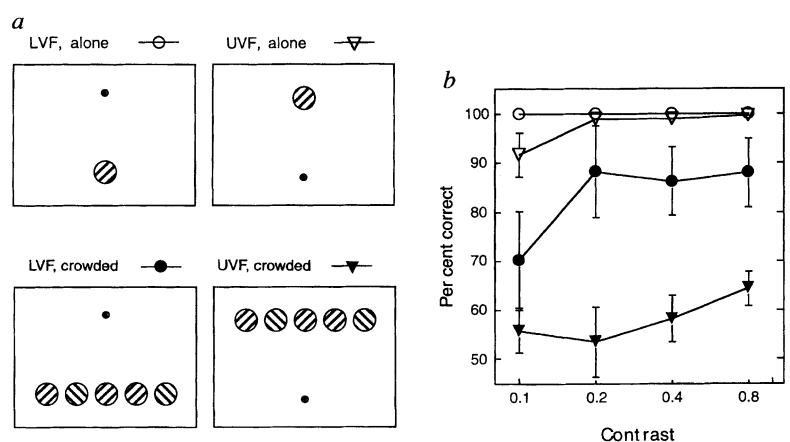
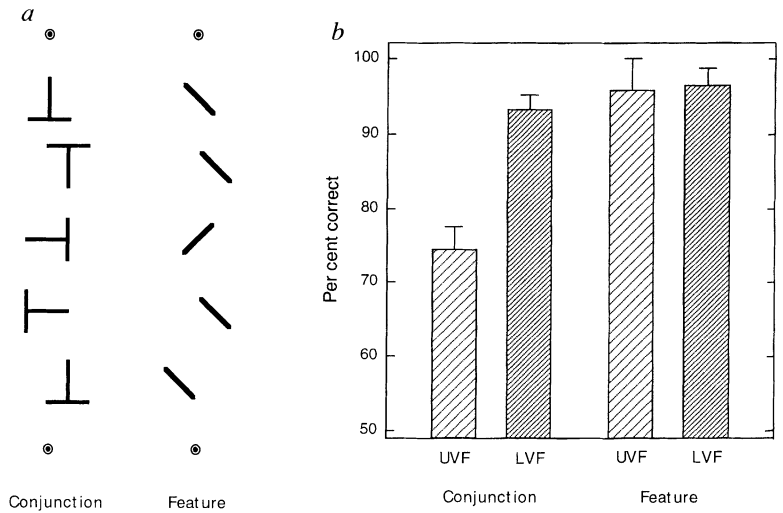


FIG. 3 *a*, Schematic examples of stimuli used in the feature detection and the conjunction detection condition. Subjects attended to the central stimulus, and responded to the presence or absence of the prespecified target (in this example, the 45° bar is the target in the feature case and the T tilted 90° clockwise is the conjunction target). Line segments in both cases subtended 2° and vertical centre-to-centre distance between elements was 3°. To reduce the contribution of global shape recognition on detection ability, the horizontal position of each element was randomly centred 1° to the left or right of the vertical midline. Stimuli were presented for 150 ms and feedback about whether the response was correct was given in each trial. *b*, Accuracy data collected in four conditions. Each bar is the mean ± s.e.m. of 4 subjects. Conjunction detection suffers a large asymmetry between upper (UVF) and lower visual field (LVF), whereas feature detection is equally good in both the upper and lower visual field.



upper and lower visual fields. Consequently, we would not expect any asymmetry in crowding effects if performance were determined principally in the primary visual cortex. To test this prediction, we compared performance in the upper and lower visual fields directly in an orientation discrimination task. Rather than maximizing the crowding effect with a radial stimulus organization<sup>5,7</sup> as in the first experiment, we arranged the stimuli horizontally to reduce crowding and to expose any modulation by visual field. The stimulus consisted of either a single grating patch or the same grating patch flanked by four similar patches, two on each side (Fig. 2*a*). The target grating was tilted either to the right (45°) or to the left (135°). Subjects were asked to fixate a point above the stimulus pattern in half of the trials, and a point the same distance below it on the other half. The stimulus was presented briefly (180 ms), and subjects were asked to press one of two keys to indicate which way the central grating was tilted, guessing if necessary. The results (Fig. 2*b*) reveal a strong asymmetry in performance: crowding reduced the accuracy of report significantly more when the target was in the upper visual field than when it was in the lower field.

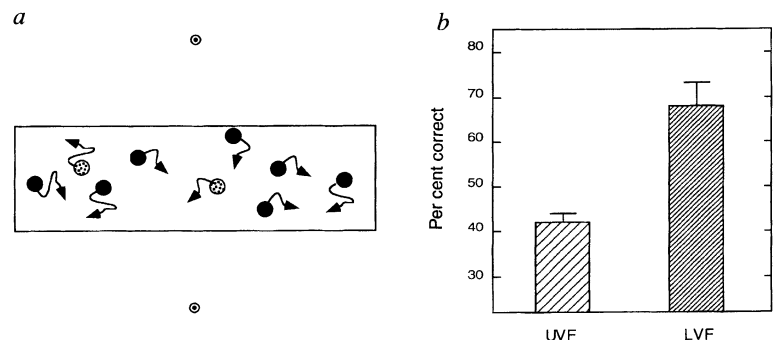
If crowding is a result of insufficient spatial resolution of attention, then performance in tasks that require more focused attention should be better when the stimulus is presented in the lower visual field than in the upper visual field, whereas tasks that demand little focused attention should show little or no asymmetry. Visual search tasks provide examples of both attentional categories. Many studies have shown that searches for feature-defined targets (where the target has the odd feature in an otherwise homogeneous array) require little focused attention, whereas searches for conjunction targets (where targets and distractors share features but differ in how they are combined) often require focused attention<sup>13</sup>. We used two simplified versions of these tasks. Five items were presented along a vertical line

above or below the point of visual fixation. In half of the trials, the item in the centre was the prespecified target, and in the other trials, the central item was a distractor. In the feature detection condition, the target was a line angled at 45° among 135° distractors, and in the conjunction detection condition, the target was a vertical and a horizontal line arranged in a 'T' shape rotated by 90° to the right, with distractors of the same shape in the three other orientations (upright, upside down, 90° rotation to the left). The target and distractors all contain the same features and are distinguished only by the conjunction of their positions (Fig. 3*a*). In the feature detection task, subjects performed equally well when targets were presented in the upper and lower visual field, whereas in the conjunction detection task, subjects showed the predicted, improved detection ability in the lower visual field (Fig. 3*b*).

Finally we used an attentional tracking task that places strong and constant demands on the attentional system<sup>14,15</sup>. Subjects were presented with 9 green discs moving randomly in a rectangular area in the upper or lower visual field. At the start of each trial, two discs were identified as targets by briefly turning red. They then turned back to green and subjects were asked to track the two targets with their attention while fixating a central dot. At the end of 5 s, all discs stopped moving and subjects were required to report which were the original targets. Tracking performance was significantly better in the lower visual field than in the upper visual field (Fig. 4).

Without distractors, perception of spatial details is limited by conventional visual resolution. However, when several items are presented, perception of the spatial details of a particular item seems to depend on the ability of attentional processes to isolate the item. This suggests that attentional resolution limits the access of spatial details to perceptual awareness. We believe that the frequently reported degradation of spatial information when

FIG. 4 Attentional tracking task and accuracy data. *a*, Subjects fixated 10° above or below the centre of a 6.6° × 30° area in which nine green moving discs were presented. At the start of each trial, two of the discs were changed to red for 1 s, and then turned back to green. Subjects were required to track these two discs with their attention while keeping their gaze steady on the fixation dot. After 5 s, all nine discs stopped moving, and subjects were asked to identify the target discs. Chance performance was 22.2%. *b*, Subjects performed much better when the discs were presented in the lower visual field. Mean ± s.e.m. of 4 subjects.



several items are present in the visual field may be a result of this limitation<sup>16,17</sup>. The asymmetry in attentional resolution between the upper and lower visual field may also contribute to the reported lower visual field advantage for the perception of global shape in tasks involving hierarchical structures where several elements are used<sup>18–20</sup>.

We attempted to locate the cortical area that mediates visual attention and limits the final access to our conscious vision. We show that stimuli not available to conscious perception could produce undiminished orientation-specific adaptation, a process that first occurs in primary visual cortex. Clearly, neuronal activity in the primary visual cortex is not sufficient for conscious percep-

tion. This is further supported by the fact that although there is little anatomical asymmetry between the upper and lower visual fields in human primary visual cortex<sup>10–12</sup>, crowding and other manipulations of attentional load produced a large asymmetry favouring the lower visual field. The same holds for V2 as well. The dorsal parietal system has classically been associated with attentional processes<sup>21,22</sup> and the projections from early visual areas to the parietal regions are more numerous for the lower visual field than the upper field<sup>23</sup>. We suggest that the dorsal parietal area may control attentional resolution and the information entering our conscious vision. □

Received 9 April; accepted 9 July 1996.

- Campbell, F. W. & Gubisch, R. W. *J. Physiol.* **186**, 558–578 (1966).
- He, S., Smallman, H. S. & MacLeod, D. I. A. *Invest. Ophthalmol. Vis. Sci. Suppl.* **36**, 2010 (1995).
- Blakemore, C. B. & Campbell, F. W. *J. Physiol.* **203**, 237–260 (1969).
- Bouma, H. *Nature* **226**, 177–178 (1970).
- Toet, A. & Levi, D. M. *Vision Res.* **32**, 1349–1357 (1992).
- Crick, F. & Koch, C. *Nature* **375**, 121–123 (1995).
- Chambers, L. & Wolford, G. *Bull. Psychonom. Soc.* **21**, 459–461 (1983).
- Kolb, F. C. & Braun, J. *Nature* **377**, 336–338 (1995).
- Chastain, G. *Psychol. Res.* **45**, 147–156 (1983).
- Horton, J. C. & Hoyt, W. F. *Archives Ophthalmol.* **109**, 816–824 (1991).
- Sereno, M. I. *et al. Science* **268**, 889–893 (1995).
- DeYoe, E. A. *et al. Proc. Natl Acad. Sci. USA* **93**, 2382–2386 (1996).
- Treisman, A. Q. J. *Exp. Psychol. Human Exp Psychol.* **40**, 201–237 (1988).
- Pylshyn, Z. W. & Storm, R. W. *Spatial Vis.* **3**, 179–197 (1988).

- Intriligator, J., Nakayama, K. & Cavanagh, P. *Invest. Ophthalmol. Vis. Sci. Suppl.* **32**, 1040 (1991).
- Butler, B. E. & Currie, A. *Psychol. Res.* **48**, 201–209 (1986).
- Taylor, S. G. & Brown, D. R. *Percept. Psychophys.* **12**, 97–99 (1972).
- Previc, F. H. *Behav. Brain Sci.* **13**, 519–575 (1990).
- Christman, S. D. *Bull. Psychonom. Soc.* **31**, 275–278 (1993).
- Rubin, N., Nakayama, K. & Shapley, R. *Science* **271**, 651–653 (1996).
- Gazzaniga, M. S. & Ladavas, E. in *Neurophysiological and Neuropsychological Aspects of Spatial Neglect* (ed. Jeannerod, M.) 203–213 (Elsevier, Amsterdam, 1987).
- Posner, M. I. *Neuropsychol. Rehab.* **4**, 183–187 (1994).
- Maunsell, J. H. & Newsome, W. T. *Annu. Rev. Neurosci.* **10**, 363–401 (1987).

ACKNOWLEDGEMENTS. We thank K. Nakayama, N. Rubin, M. Chun, C. Moore, F. Verstraten and C. Koch for useful discussions. This work was supported by NIH grants to S.H. and P.C.

CORRESPONDENCE and requests for materials should be addressed to S.H. (e-mail: Sheng@wjh.harvard.edu).

## Homodimeric architecture of a CIC-type chloride ion channel

Richard E. Middleton, Deborah J. Pheasant & Christopher Miller

Howard Hughes Medical Institute, Graduate Department of Biochemistry, Brandeis University, Waltham, Massachusetts 02254, USA

**THE recent discovery of the CIC-family of anion-conducting channel proteins<sup>1–3</sup> has led to an appreciation of the central roles played by chloride ion channels in cellular functions, such as electrical behaviour of muscle<sup>4–7</sup> and nerve<sup>8</sup> and epithelial solute transport<sup>9</sup>. Little is known, however, about molecular architecture or sequence–function relationships in these membrane proteins. In the single case of CIC-0, a voltage-gated ‘muscle-type’ chloride channel, the functional complex is known to be a homo-oligomer of a polypeptide of  $M_r \sim 90,000$ , with no associated ‘helper’ subunits<sup>10</sup>. The subunit stoichiometry of CIC-type channels is controversial, however, with either dimeric or tetrameric association suggested by different indirect experiments<sup>10,11</sup>. Before a coherent molecular view of this new class of ion channels can emerge, the fundamental question of subunit composition must first be settled. We have examined hybrid CIC-0 channels constructed from functionally tagged subunits, and report here that CIC-0 is a homodimer containing two chloride-conduction pores.**

These experiments examine CIC-0 channels purified and functionally reconstituted after high-level heterologous expression in mammalian cells. The expressed channels display the same molecular and functional characteristics observed<sup>10</sup> with CIC-0 purified from its natural source, *Torpedo* electroplax (Fig. 1). Both preparations run identically on sodium dodecyl sulphate-polyacrylamide gel electrophoresis (SDS–PAGE) gels as single, lightly glycosylated 90K bands; the expressed, purified channels incorporated into planar lipid bilayers show the same single-channel conductance and voltage-dependent gating behaviour

as the native *Torpedo* channel<sup>12–14</sup>. An unusual characteristic of CIC-0 channels—and one essential to grasp for addressing questions of molecular structure—is the existence of two identical and physically separate Cl<sup>–</sup>-conduction pores in a ‘double-barrelled’ complex<sup>12–16</sup>. This feature is manifested in the single-channel records by three distinct, equally spaced conductance levels, in which the pores are either both closed (level 0), one open and one closed (level 1), or both open (level 2). Because the two pores are identical, level 1 is degenerate, the conductance being the same regardless of which pore is open.

Recently, residue K519, putatively located on the cytoplasmic side of the membrane just after the twelfth transmembrane domain, was found by macroscopic electrophysiological experiments to influence gating and anion permeation<sup>17</sup>. The single-pore conductance is sensitive to the charge at this position (Fig. 2). Similar conductances are seen for K519 ( $16.1 \pm 1$  pS) and R519 ( $13.1 \pm 0.3$  pS), whereas electrically neutral substitutions, regardless of their chemical nature (C519, Q519, M519, F519), yield channels with about half this conductance (5–7 pS). Substitution of a negative residue lowers the conductance further (2–3 pS). The dependence of conductance on side-chain charge argues that the residue influences Cl<sup>–</sup> permeation primarily by an electrostatic mechanism. A small but statistically significant effect of side-chain volume may also operate because the R519 conductance is lower than that of K519 and the F519 conductance falls below those of the smaller neutral replacements. All these charge-substituted channels display the three binomially distributed gating levels of the double-barrelled channel complex<sup>12,13</sup>, in which level 2 has precisely twice the conductance of level 1. The preferential effect of charge substitutions on inward current (Fig. 2b and ref. 17) indicates that residue 519 might be located on the cytoplasmic side of the channel, a weak suggestion that we unambiguously confirm below.

The single-channel conductance can be used as a functional tag in subunit-mixing experiments to deduce the number of CIC-0-519 residues contributing to the pore, and hence the number of subunits in the homo-oligomer. We coexpressed complementary DNAs coding for K519 and C519, purified the resulting channels, and examined the single-channel permeation properties of these